Morphological characterization of ABS and PC-ABS surfaces for automotive industry

Gianluca Deninno[1], Ettore Vittone[1], Nello Li Pira[2], Fabio Scaffidi Muta[2], Luca Belforte[2] and Renzo Costa[2]

[1] *University of Turin, Department of physics, Via Pietro Giuria, 1, 10125 Turin, Italy*
[2] *CRF - Materials Engineering Methods Tools, C.so Settembrini 40, 10135 Turin – Italy*

gianluca.deninno@edu.unito.it

Abstract—In the automotive industry, the measurement, control and reproducibility of certain morphological characteristics of surfaces are important to characterize, qualify, certify and optimize different physical properties, such as the degree of wear, the degree of adhesion by adhesives, glues or paints and optical properties. In this regard, this work wants to demonstrate how it is possible to characterize different surfaces in ABS (Acrylonitrile Butadiene Styrene) and PC-ABS (PolyCarbonate/Acrylonitrile Butadiene Styrene) material through a new set of morphological parameters defined according to the ISO 25178 standard. These particular surfaces have been subjected to different etching treatments performed with different chemical elements: these treatments can radically modify the morphology of the surface, making it more or less suitable according to the industrial purposes sought. At the end of the paper, the correlation between the *Sdq* and *Sdr* parameter for this type of surfaces will be studied and a theoretical relationship between this morphological parameters will also be proposed. This study is based on the use of a DCM8 confocal optical microscope and a SEM (Scanning Electron Microscope), which allow to obtain surface morphological information on a micrometric and nanometric scale and the measurements obtained are analyzed with special imaging and three-dimensional scanning software that allow the precise measurement of morphological parameters of the standard ISO-25178.

Keywords— ISO-25178, ABS, PC-ABS, Beckmann distribution, morphological parameters, *Sdq* and *Sdr* correlation.

I. INTRODUCTION

In recent years, the development of a method to study textured surfaces has been essential as it can explain a large number of physical properties often required for industrial purposes, such as anti-corrosive, hydrophobic, hydrophilic and anti-freeze properties [1–4]. A precise surface characterization is increasingly required in many industrial fields, from aerospace to photovoltaic industry, making a morphological characterization method indispensable [5, 6]. Even the optical properties of a surface can strongly depend on the morphology: the perceived optical effect, which is often described in the literature through the BRDF (Bidirectional Reflectance Distribution Function), is influenced by the distribution of the normal unit vectors of the surface itself, as well as by its morphology [7–15].
The ISO 25178 standard series of the Geometrical Product Specifications (GPS) system proposes a structured method for the characterization of the surface texture. In this standard, many morphological parameters are defined. These parameters describe particular characteristics of a surface and are calculated on the morphology measured through contact and non-contact instruments. This standard also defines several morphological filters, defined in the wavelength space, which through the calculation of the Fourier transform allow for example to remove measurement errors that arise during the surface acquisition of the studied sample.
In this work several results about a restricted number of these parameters will be shown, studied and described: these parameters are able to provide a precise description of the surface morphology and through them it will be shown how it is possible to characterize a surface for many practical industrial aspects.
The main purpose of this work is to show how it is possible to qualify ABS and PC-ABS surfaces through the ISO 25178 standard. In this paper, surfaces in ABS and PC-ABS material etched through chemical baths based on hexavalent chromium are studied. In many industrial application fields, etching baths are based on this particular chemical element but several technologies have been advanced to avoid using hexavalent chromium. Therefore, this article also shows the morphological differences of surfaces etched through hexavalent chromium or through other chemical elements. The main parameter that in this work characterizes the process of etching is the time of immersion: the main morphological differences as a function of the time of immersion will

be shown, explaining which surfaces have similar morphologies depending on the type of material and process of etching used.

II. STANDARD DEFINITIONS

The parameters of the ISO 25178 standard can be divided into height parameters, volume parameters, hybrid parameters, and functional parameters. In this section, the definitions of the morphological parameters used are shown and additional definitions are provided.

The definitions shown are extended to the continuous case. The studied surface is immersed in a Cartesian reference system and it is parameterized through the graph of a two-dimensional function $f(x,y) : \mathbb{R}^2 \to \mathbb{R}$ of class C^1: in this way, it is possible to obtain the coordinates (x,y,z) of all the measured points through the Cartesian surface

$$\vec{S_\Sigma} = (x, y, f(x,y)) \qquad (1)$$

where the x-axis and y-axis represent respectively the longitudinal and transverse axes of the measured surface. The mean $\overline{f}(x,y)$ of the function $f(x,y)$ appearing in relation (1) is equal to 0, i.e. $\overline{f}(x,y) = 0$.

Heights parameters

The definitions of the height parameters are given in the following sections.

1. Sq

The *Sq* parameter is the root mean square of heights of the measured points and it is defined as

$$Sq = \sqrt{\frac{1}{A} \int \int_A f^2(x,y)dxdy} \qquad (2)$$

where A is the sampling area.

2. Sz

The *Sz* parameter is defined as

$$Sz = f_{MAX}(x,y) - f_{min}(x,y) \qquad (3)$$

where $f_{MAX}(x,y)$ and $f_{min}(x,y)$ are respectively the maximum and the minimum value of the function $f(x,y)$.

3. Ssk

The *Ssk* is the skewness parameter and it is the ratio of the mean of the height values cubed and the cube of *Sq* parameter

$$Ssk = \frac{1}{Sq^3}\frac{1}{A} \int \int_A f^3(x,y)dxdy \qquad (4)$$

The values of the *Ssk* can be positive, negative or zero, and is unit-less since it is normalised by *Sq*.

4. Sku

The *Sku* parameter is defined as the ratio of the mean of the fourth power of the height values and the fourth power of *Sq*

$$Sku = \frac{1}{Sq^4}\frac{1}{A} \int \int_A f^4(x,y)dxdy \qquad (5)$$

As the skewness parameter, the *Sku* parameter is unit-less and the values it can assume are strictly positive.

Hybrid parameters

5. Sdq

Through the definition of the Cartesian surface shown in the equation (1), it is possible to calculate the gradient of the surface for any points of the surface. The *Sdq* parameter is defined as the root mean square of gradient and it is calculated as

$$Sdq = \sqrt{\frac{1}{A} \int \int_A \left(f_x^2 + f_y^2\right)dxdy} \qquad (6)$$

where the used quantities f_x and f_y are respectively the partial derivative of $f(x,y)$ calculated along the x-axis and y-axis.

6. Sdr

The *Sdr* parameter is the developed interfacial area ratio and it is defined as

$$Sdr = \frac{1}{A} \int \int_A \left(\sqrt{1 + f_x^2 + f_y^2} - 1\right)dxdy \qquad (7)$$

Also the *Sdr* parameter, as the *Sdq* parameter, is dimensionless.

Volume parameters

7. Vv

The *Vv(mr)* parameter, the Void Volume, is the volume of space bounded by the surface texture from a plane at a height corresponding to a chosen *material ratio* value to the lowest valley. The "mr" value may be set to any value from 0% to 100%: the *Vv* parameter value will be maximum at $mr = 0\%$ and minimum at $mr = 100\%$.

8. Vvc

$Vvc(p,q)$, the Core Void Volume, is the volume of space bounded by the texture at heights corresponding to the material ratio values of "p" and "q". The default value for "p" is 10% and the default value for "q" is 80%. This parameter is useful to evaluate the empty space between the walls of the surface in a 'central' range of heights.

Distribution of normals

In this section, the definition of the distribution of normals widely used in the literature for the evaluation of surfaces is shown. For each measured point of the studied surface, its unit normal vector $\hat{w}$ can be calculated and can be described by spherical coordinates (θ, φ) as

$$\hat{w}(\theta, \varphi) = (\sin\theta\cos\varphi, \sin\theta\sin\varphi, \cos\theta) \qquad (8)$$

If the coordinates θ and φ are known for all measured points, then the distribution of these coordinates can be calculated: this distribution is the distribution of normals $D(\theta, \varphi)$ and it is measured in $[\text{m}^2 \cdot \text{st}^{-1}]$, where st indicates steradian. Extending the definition to the continuous case, the distribution of the normals is defined in such a way that the portion

of area $dS_\Sigma(\Omega)$ of the surface $\vec{S_\Sigma}$ indicated in equation (1), whose unit vectors have spherical coordinates between the solid angle Ω and $\Omega + d\Omega$, can be calculated as

$$
\begin{aligned}
dS(\Omega) &= D(\Omega)d\Omega \\
&= D(\theta,\varphi)\sin\theta d\theta d\varphi
\end{aligned}
\tag{9}
$$

The whole area S_Σ of the Cartesian surface $\vec{S_\Sigma}$ can then be calculated by integrating the relation (9) in the hemisphere of the solid angle Ω_+, in which the normal unit vectors have the third Cartesian component always positive. In the literature, the distribution of normals is normalised so that the area of the projection of the surface $\vec{S_\Sigma}$ on the x-y plane, i.e. the sampling area, has an area equal to 1 m^2, i.e.

$$
\int_{\Omega_+} D(\theta,\varphi)\sin\theta\cos\theta d\theta d\varphi = 1 \quad [m^2] \tag{10}
$$

III. MEASUREMENT METHOD

This section shows the procedure used to calculate the ISO 25178 morphological parameters. The calculation of the parameters is obtained through the software Leica, called *Mountains Map*. This software allows to analyze the images obtained both by confocal microscope and SEM. It also allows the application of different morphological filters to the measurements obtained in order to obtain the most representative parameter measurements.
This procedure is divided into the following steps:

1. Obtain the measurement of surface morphology by confocal microscope. This measurement contains the Cartesian coordinates (x, y, z) of all points measured by the optical instrument;

2. In case the area obtained from the measurement does not have a square area, or in case a smaller portion of the area wants to be evaluated, cut out a square portion of the measured area. The obtained portion of square area $l \times l$ will be used for the calculation of morphological parameters;

3. Apply S filter. A low-pass filter is applied to the square area obtained: this filter has a nesting index equal to S_1. In this way, the primary coordinate surface (x_S, y_S, z_S) is obtained. This value is a function of the maximum sampling distance and eliminates small-scale components of the surface. The S_1 filter nesting index is determined according to the recommendations of the ISO 25178-3:2012;

4. Remove the form. It can often happen that the sample is not perfectly perpendicular to the optical axis of the confocal microscope, causing errors in the calculation of morphological parameters. Therefore, in this work the shape has always been removed through a geometric plane: this plane is calculated through the method of least squares and the value that this plane takes in the x and y coordinates of the measured points has been subtracted from the z coordinates of each point. In this way, the S-F surface of coordinates (x_{SF}, y_{SF}, z_{SF}) is obtained.

All morphological parameters calculated and shown in this paper are obtained from the S-F surfaces obtained from each measurement. The S-F surfaces used have $l = 40$ μm and a nesting index $S_1 = 0.8$ μm has been chosen for all samples studied.
The confocal microscope used for all measurements is the Leica DCM8 and the objective used for the measurements is a 150X. Table 1 shows schematically the characteristics of the optical lens used.

Bright field Objectives	NA	Spatial Sampling [μm]	Optical Resolution [μm]
150X	0.95	0.09	0.14

TABLE 1: GENERAL SPECIFICATIONS OF THE 150X OBJECTIVE OF LEICA DCM8 CONFOCAL MICROSCOPE.

IV. VALIDATION OF THE SOFTWARE

Before proceeding with the measurements through the confocal microscope and the calculation of morphological parameters, the goodness of the software used was verified. To do this, a reference data sets were used [16]. This site is made available by NIST (National Institute of Standards and Technology) on their Internet based Surface Metrology Algorithm Testing System and it is possible to find different maps of surfaces with particular morphological characteristics. The maps SG_1-1, SG_1-2, SG_1-3, SG_1-4, SG_2-1, SG_2-3, SG_3-1 and SG_3-2 have been downloaded and for each of these have been calculated through the software used the height parameters: these results were then compared with the reference results provided by the site.
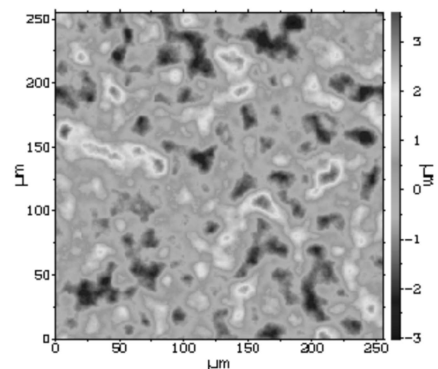

Fig. 1: An example of map used to evaluate the goodness of software: in this case, the SG_1-2 downloaded from the website of NIST is shown.

Going into greater detail, for each surface downloaded from the database, the height parameters were calculated[1]. Subsequently, a graph was obtained for each parameter studied, where the values of the parameters obtained and measured with the software used have been reported on the x-axis and the values of the parameters provided by the site have been reported on the y-axis. In this way, if the software used worked correctly, the expected best fit that correlates the measured parameters with the parameters provided by the

---

[1] The parameter *Sq*, *Sp*, *Sv*, *Ssk* and *Sku* were calculated.

NIST is a linear fit of the type $y = mx + q$ whose angular coefficient m is compatible with 1 and the intercept q with 0.

An explanatory example is reported to make this procedure clearer. For each of the downloaded surfaces[2], the Ssk parameter was calculated with the software used. The eight measured values of Ssk were then obtained and each of these was reported on the x-axis of a graph. Similarly, the Ssk parameter values corresponding to the relevant maps provided by NIST were plotted on the y-axis. The result obtained for the Ssk parameter is shown schematically in figure 2.
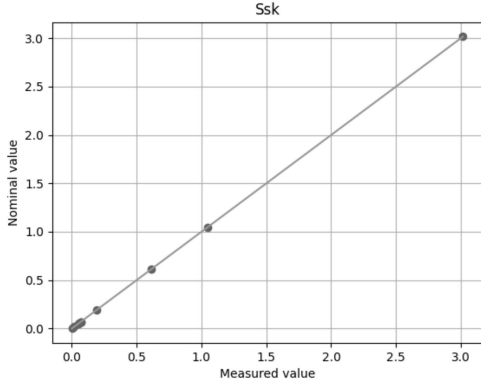

Fig. 2: On the x-axis, the Ssk values measured by the software used were reported and on the y-axis the values of the parameter provided by the website of NIST were plotted.

At this point, the intercept and angular coefficient of the best fit shown in the figure 2 via an orange line have been calculated. In this case, the values are[3]

$$\begin{cases} m = (1.00009 \pm 0.00016) \\ q = (-16 \pm 18) \cdot 10^{-5} \end{cases} \qquad (11)$$

As expected both values obtained about the angular coefficient and the intercept are compatible with 1 and 0 respectively: this consideration was decided to be sufficient to consider reliable the values of the Ssk parameter calculated by the software used.

This procedure is repeated for Sq, Sp, Sv and Sku parameters using unfiltered surfaces. The results obtained about the best fit parameters are shown schematically in table 2. For the tables 2 and 3, the values of q and their errors for the morphological parameters of Sq, Sp and Sv are reported in [μm]. The same type of work was similarly obtained for filtered surfaces with nesting index $S_1 = 0.008$ mm made available from the same website. The results obtained about the best fit parameters are shown schematically in table 3.

Parameters	m	σ_m	q	σ_q
Sq	0.9999999	$2 \cdot 10^{-7}$	$9 \cdot 10^{-7}$	$5 \cdot 10^{-7}$
Sp	1.0000004	$5 \cdot 10^{-7}$	$-4 \cdot 10^{-7}$	$2 \cdot 10^{-7}$
Sv	0.9999998	$4 \cdot 10^{-7}$	$3 \cdot 10^{-7}$	$2 \cdot 10^{-7}$
Ssk	1.00009	$16 \cdot 10^{-5}$	$-16 \cdot 10^{-5}$	$18 \cdot 10^{-5}$
Sku	1.000007	$8 \cdot 10^{-6}$	$-15 \cdot 10^{-6}$	$6 \cdot 10^{-6}$

TABLE 2: PARAMETERS ABOUT THE BEST FIT OBTAINED FOR UNFILTERED MAPS ARE SHOWN.

[2]In this example, unfiltered map was downloaded.

[3]In this case, both parameters obtained are dimensionless.

Parameters	m	σ_m	q	σ_q
Sq	1.0000002	$2 \cdot 10^{-7}$	$5 \cdot 10^{-7}$	$3 \cdot 10^{-7}$
Sp	0.9999999	$5 \cdot 10^{-7}$	$3 \cdot 10^{-7}$	$3 \cdot 10^{-7}$
Sv	1.0000007	$8 \cdot 10^{-7}$	$-3 \cdot 10^{-7}$	$2 \cdot 10^{-7}$
Ssk	1.00004	$9 \cdot 10^{-5}$	$-3 \cdot 10^{-5}$	$5 \cdot 10^{-5}$
Sku	0.99998	$12 \cdot 10^{-5}$	$2 \cdot 10^{-5}$	$4 \cdot 10^{-5}$

TABLE 3: PARAMETERS ABOUT THE BEST FIT OBTAINED FOR FILTERED MAPS WITH NESTING INDEX $S_1 = 0.008$ mm ARE SHOWN.

All parameters about the best fit obtained are compatible with the expected value using a confidence interval of 3σ: this observation was considered sufficient condition to consider the software used reliable.

V. ABS SURFACE MEASUREMENTS

The samples of ABS surfaces studied are six. This set of samples is divided into two groups: 3 samples have been subjected to an etching treatment through chemical baths based on hexavalent chromium, while the other 3 have been subjected to a similar treatment but without using hexavalent chromium. Within each of these two groups, there are three types of samples: the "$Under$" sample, indicating that the immersion time inside the chemical bath is 5 minutes, that is a time relatively low, the "$Standard$" sample, whose for the samples studied the immersion time is 10 minutes and the "$Over$" sample, whose immersion time is relatively high, for immersion times between 15 and 20 minutes.

The measurements on ABS samples were made using the microscope and optical objective whose specifications are schematically shown in table 1 and the measurement of morphological parameters for each sample was performed as follows. For each sample, 3 different S-F surfaces were obtained: for each of them, the morphological parameters were calculated. The best estimate of the morphological parameter of the sample was decided to be the average of the 3 parameters obtained, while the error associated was decided to be the semi-dispersion of the 3 measurements.

The samples subjected to an etching treatment where hexavalent chromium has not been used are called "Evolve" samples, a term used to refer to the new industrial etching treatment and samples etched through the use of hexavalent chromium were called "Cr6".

In a similar way, the legend for each graph in this section refers to samples etched with hexavalent chromium as "Cr6", and to samples etched without hexavalent chromium as "Evolve".

Table 4 summarises schematically the names of the samples used and the time of immersion of the etching process.

ABS, Immersion of time [min]					
"Cr6"			"Evolve"		
Under	_Standard_	_Over_	_Under_	_Standard_	_Over_
5	10	15	5	10	20

TABLE 4: THE NAMES USED FOR THE SAMPLES AND THE TIMES OF IMMERSION, EXPRESSED IN MINUTES, ARE SHOWN.
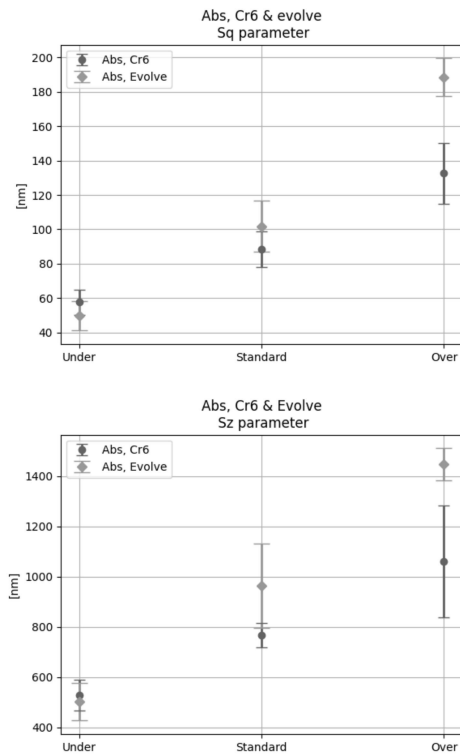
Fig. 3: On the top, the *Sq* measurements are shown. On the bottom, the *Sz* measurements are reported.

Comparison of etching process

In this section, results obtained for ABS surfaces etched through hexavalent chromium and "Evolve" samples are compared.

1. Height parameters

The parameters *Sq* and *Sz* are shown schematically in figure 3, while the parameters *Ssk* and *Sku* are reported schematically in figure 4: in both images, the measurements made on the Evolve samples are shown in orange and the surfaces etched through hexavalent chromium in blue. As can be observed from figure 3, both *Sq* and *Sz* increase with increasing immersion time: this statement is valid for samples etched with hexavalent chromium as well as for Evolved samples. From the same figure, it is possible to observe that the parameters are not compatible for immersion times longer than 10 minutes. This observation may be consistent with what has been observed from the images acquired with the SEM: the difference can be appreciated by observing the images of figure 16 and 17, in which ABS surfaces etched through hexavalent chromium and through Evolve baths, respectively, are schematically shown.

The *Ssk* and *Sku* parameters are instead shown schematically in figure 4, where for both images the measurements about the Evolve samples are shown in orange and the samples etched through hexavalent chromium in blue. As the *Ssk* parameter is defined, it assumes a zero value if the distribution of the heights of the measured points is a normal distribution, it assumes negative values if there is a predominance of valleys and assumes positive values if, on the contrary, there is a predominance of peaks. It is possible to observe from

figure 4 that the *Ssk* parameter for ABS surfaces etched with hexavalent chromium has an almost constant trend and for high immersion times the *Ssk* value approaches zero. For this type of samples, therefore, the distribution of heights becomes slightly more symmetrical with high immersion times, which makes the presence of valleys and peaks more homogeneous. On the contrary, for Evolve samples made of ABS material, the *Ssk* parameter decreases with increasing the time of immersion, showing that in this case the etching process causes larger and deeper valleys in the sample morphology. This observations are consistent comparing the images obtained by SEM: as shown schematically in figure 16, the valleys that characterize "*Under*" samples etched with hexavalent chromium gradually become less and less distinguishable due to higher immersion times, contrary to what happens on the "Evolve" samples, where larger and deeper valleys are more visible for longer times of immersion, as shown in the lower image of figure 17.
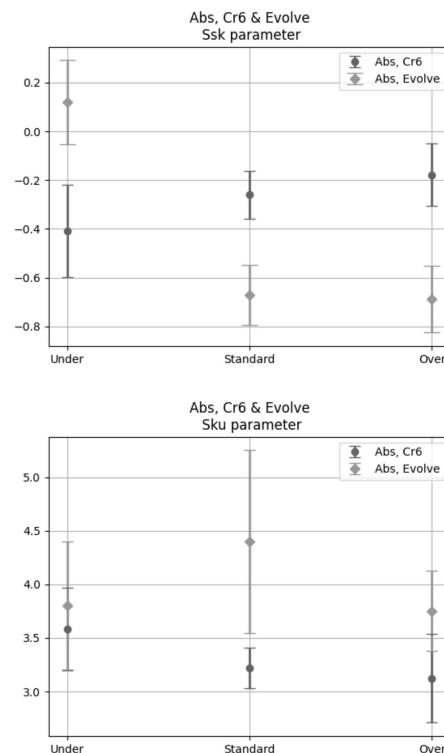

Fig. 4: On the top, the *Ssk* measurements are shown. On the bottom, the *Sku* measurements are reported.

More difficult considerations can be made instead for the *Sku* parameter. As schematically shown in the lower picture of 4, the uncertainties associated with measurements of this parameter are relatively high. Both the *Ssk* and *Sku* parameters are defined by higher order powers of the heights of the measured points and this can increase the error of the measurements of these parameters: for this reason, it is often necessary to conduct several measurements for a more precise estimate of these two parameters. In any case, by definition, the *Sku* parameter assumes values greater than 3 for morphologies characterized by very high peaks and particularly deep valleys: in fact, this parameter is often used to characterize surfaces subject to abrasion and corrosion.

2. Hybrid parameters

The *Sdq* and *Sdr* parameters are shown schematically in figure 5. Similarly to the previous images, measurements about surfaces etched through hexavalent chromium are shown in blue, while Evolve surfaces are shown in orange. The hybrid parameters also increase with increasing immersion time of the samples, regardless of the type of etching. In general, the values of the *Sdq* and *Sdr* parameters are high for complex and irregular morphologies and assume lower values for smoother surfaces. Observing figure 5, it is also possible to note that, for immersion times longer than 10 minutes, the *Sdq* and *Sdr* parameters are compatible for ABS surfaces.
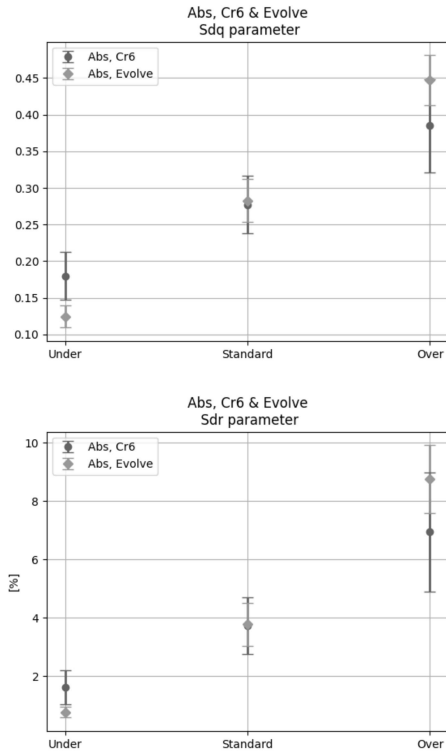
Fig. 5: On the top, the *Sdq* measurements are shown. On the bottom, the *Sdr* measurements are reported.

3. Volume parameter

The *Vv* and *Vvc* parameters are schematically shown in figure 6. The measurements for ABS surfaces etched with hexavalent chromium are shown in blue, while the measurements obtained with Evolve samples are shown in orange. The *Vv* parameter is a parameter normalised to the measured area and for the measurements shown in this section it was calculated with a material ratio value of $mr = 10\%$. Similarly, the *Vvc* parameter was calculated with the values of p and q set at 10% and 80% respectively.

As can be seen from figure 6, these two parameters are compatible for immersion times of less than 10 minutes, regardless of the type of chemical bath: for longer immersion times, the *Vv* and *Vvc* parameters for the Evolve surfaces, however, are larger than the parameters measured on surfaces etched with hexavalent chromium. This statement implies that etching with long immersion times on ABS surfaces causes a larger void volume between the walls of the observed surface

morphologies than observed on ABS surfaces etched with hexavalent chromium.
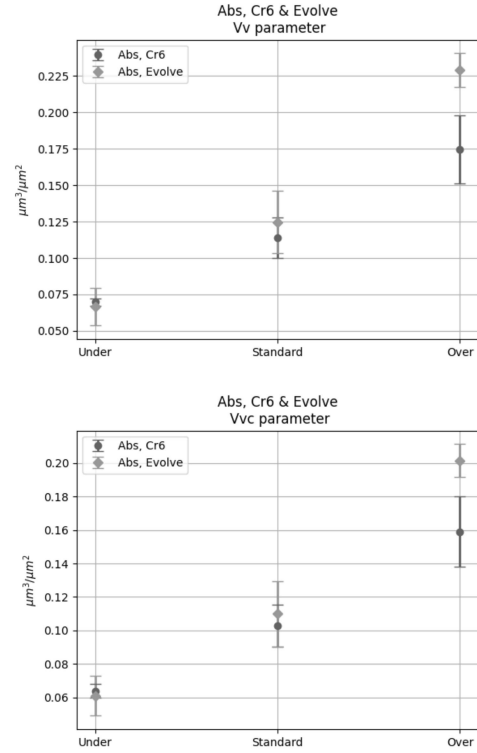

Fig. 6: On the top, the *Vv* measurements are shown. On the bottom, the *Vvc* measurements are reported.

VI. PC-ABS SURFACE MEASUREMENTS

Similarly to the ABS surfaces, the PC-ABS samples studied are six. These six samples are divided into two groups: 3 samples were etched using a chemical bath based on hexavalent chromium, while the other 3 were etched using the "Evolve" etching process, i.e. without using hexavalent chromium. Each of the two groups has a sample called "*Under*", which indicates an etching time between 6 and 8 minutes, a sample called "*Standard*" and a sample called "*Over*", which indicates a higher etching time, in this case between 18 and 25 minutes depending on the sample. Table 5 schematically shows the names used for the samples studied with the immersion times regarding the etching process.

PC-ABS, Immersion of time [min]					
"Cr6"			"Evolve"		
Under	*Standard*	*Over*	*Under*	*Standard*	*Over*
6	12	18	8	15	25

TABLE 5: THE NAMES USED FOR THE SAMPLES AND THE TIMES OF IMMERSION, EXPRESSED IN MINUTES, ARE SHOWN.

The measurements on PC-ABS samples were made using the microscope and optical objective whose specifications are schematically shown in table 1 and the morphological parameters for the PC-ABS samples were calculated in a similar way to the ABS surfaces: for each of the samples studied, 3 maps were measured through the confocal microscope. For each of these maps, it was possible to obtain the corre-

sponding S-F surfaces according to the procedure illustrated schematically in section III: the best estimate of the morphological parameters relative to a sample was decided to be the average of the three maps obtained and the associated error was calculated as the semi-dispersion of the three measurements.

Comparison of etching process

In this section, the results obtained for PC-ABS surfaces etched through hexavalent chromium and "Evolve" samples are shown.

1. Height parameters

Similarly for the ABS samples, the main results obtained about the height parameters for PC-ABS surfaces are shown in this section. In figure 7, the measurements of the Sq and Sz parameters are schematically shown: for each graph reported, a comparison can be observed between the parameters measured on the hexavalent chromium-etched surfaces, shown in blue, and the Evolve surfaces, shown in orange. As shown in the image at the top of figure 7, the Sq parameter is not compatible for any immersion time. In more detail, the Sq parameter increases significantly more for samples etched using hexavalent chromium, regardless of the immersion time to which the surface has been subjected.

Similarly to the Sq parameter, the Sz parameter, defined as the maximum surface height, i.e. the difference between the maximum and minimum measured height of surface, is also found to increase more for surfaces etched with hexavalent chromium.
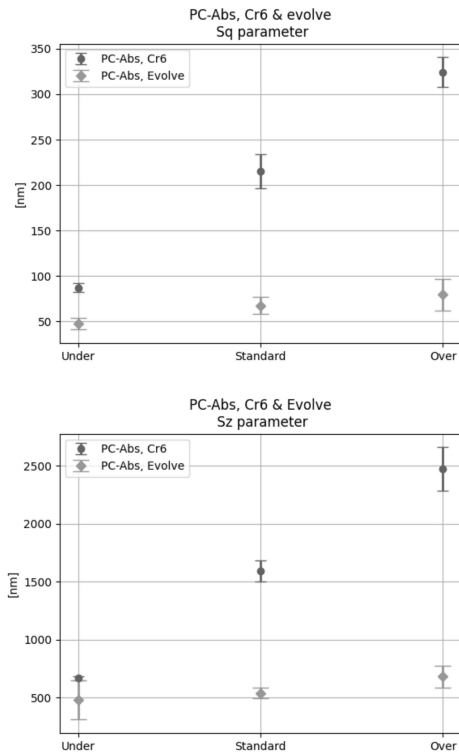

Fig. 7: In the image above, the Sq parameter measurements are shown. In the bottom image, the measurements of Sz are shown.

These observations seem to be consistent observing the im-

ages obtained through the electron microscope of the PC-ABS surfaces shown schematically in figures 18 and 19. For both figures, the samples etched with a low immersion time are shown at the top, while the samples etched with a high immersion time are shown at the bottom and the figures are shown at the same magnification: as shown in the images, the effect obtained with a longer immersion time through hexavalent chromium etching is more evident than the "Evolve" etching baths, which increases more the dispersion of the distribution of heights, and consequently the values of Sq and Sz parameter.

A similar study has been done for the Ssk and Sku parameters, shown schematically in figure 8. By definition of Ssk parameter, as described in section V, it is less than zero if the morphology observed has a predominance of valleys, while it is equal to zero if the heights of the points measured are normally distributed around a mean value. As shown in the image at the top of figure 8, the Ssk parameter is always less than zero for both hexavalent chromium-etched and Evolve surfaces.
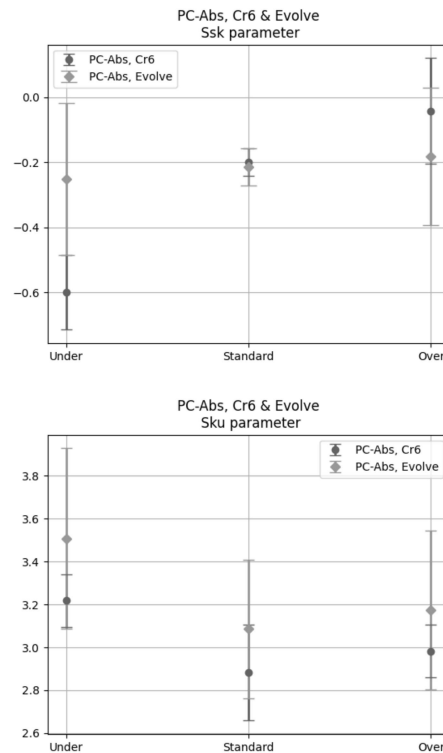

Fig. 8: In the image above, the Ssk parameter measurements are shown. In the bottom image, the measurements of Sku are shown.

As for ABS surfaces, the value of Ssk parameter for PC-ABS surfaces etched with hexavalent chromium increases with time of immersion, showing that it is more difficult to observe a predominance of surface valleys as the immersion time increases. On the contrary, for the Evolve surfaces, the Ssk parameter is slightly lower than zero, but almost constant as a function of immersion time, showing a slight predominance of valleys that remains constant regardless of immersion time. These observations are again confirmed by the images obtained through SEM, schematically shown in figures 18 and 19. Figure 18 shows the images of the surfaces etched with hexavalent chromium: as can be seen, the predominance of the valleys disappears as the immersion time increases, as

the morphology presents new peaks that are created during the etching process. Similarly, in figure 19, the images of the Evolve surfaces are shown schematically: as can be seen, the predominance of valleys remains almost constant as confirmed by the *Ssk* measurements.

The *Sku* parameter for both hexavalent chromium-etched and Evolve surfaces is compatible with 3 for etching times longer than 12 minutes ("*Standard*" and "*Over*" samples). These measurements can be interpreted from the definition of this parameter, which assumes values close to 3 when no very high single peaks or very deep single valleys are present along the observed morphology: this observation is also confirmed by the SEM images, through which no particularly very high or very deep singularities are present. As with the parameters measured on the ABS surfaces, the errors associated with the measured values are particularly high and therefore a greater number of measurements may be required to decrease the error associated.

2. Hybrid parameters

The *Sdq* and *Sdr* parameters for PC-ABS surfaces are schematically shown in figure 9. The measurements about surfaces etched through hexavalent chromium are shown in blue, while Evolve surfaces are shown in orange. Similarly to the measurements of the *Sq* and *Sz* parameters, the *Sdq* and *Sdr* parameters also differ significantly as a function of immersion time and the values of *Sdq* and *Sdr* are greater for surfaces etched with hexavalent chromium than for Evolve surfaces.
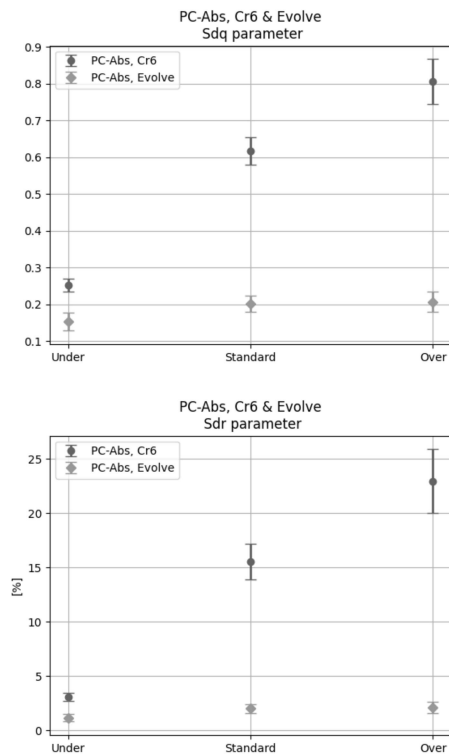

Fig. 9: In the image above, the *Sdq* parameter measurements are shown. In the bottom image, the measurements of *Sdr* are shown.

In addition, the *Sdq* value measured on surfaces etched with hexavalent chromium, as well as the *Sdr* value, is not compatible with that measured on the Evolve samples regardless

of immersion time, as can be seen from the comparison of the measurements shown in figure 9. This statement is again confirmed by the images acquired through the electron microscope, where hexavalent chrome-etched surfaces are more irregular than Evolve surfaces. These results can be useful as *Sdq* and *Sdr* are often useful in applications involving surface coatings and adhesion and both parameters find relevance when considering surfaces used with lubricants and other fluids [17].

3. Volume parameter

The *Vv* and *Vvc* parameters are schematically shown in figure 10. The measurements for PC-ABS surfaces etched with hexavalent chromium are shown in blue, while the measurements obtained with Evolve samples are shown in orange. In this section, the *Vv* parameter was calculated with a material ratio equal to $mr = 10\%$. Similarly, also for the PC-ABS measurements, the *Vvc* parameter was calculated with the values of $p = 10\%$ and $q = 80\%$.
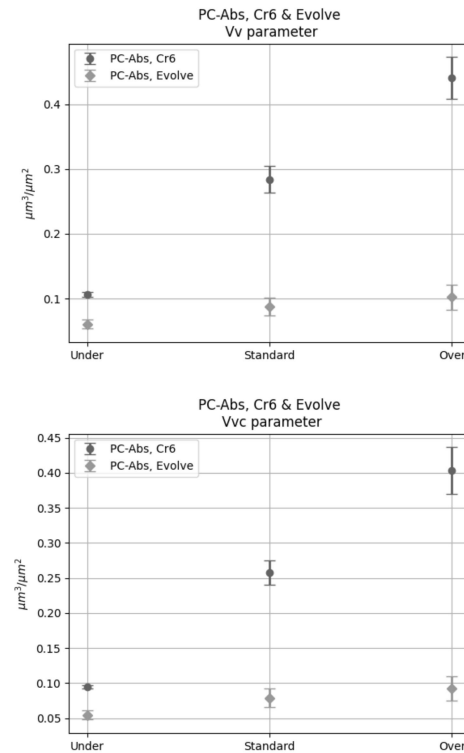

Fig. 10: In the image above, the *Vv* parameter measurements are shown. In the bottom image, the measurements of *Vvc* are shown.

The *Vv* and *Vvc* parameters measured on surfaces etched with hexavalent chromium are not compatible with parameters measured on Evolve samples independently of the immersion time. Furthermore, for surfaces etched with hexavalent chromium, both volume parameters are significantly larger than the parameters measured on the Evolve surfaces and this difference becomes greater as the immersion time increases.

These parameters, as the hybrid parameters, are often useful for qualifying surfaces for degree of adhesion by paints or glues.

VII. ABS AND PC-ABS COMPARISON

In this section, a summary and general comparison of the measurements obtained are shown. The comparison of the measurements of the *Sq*, *Sdq* and *Vv* parameters for all samples studied are shown in figures 11, 12 and 13 respectively. The PC-ABS surfaces etched with hexavalent chromium have the highest parameter values of the all parameters shown, regardless the time of immersion, as shown in figures 11, 12 and 13. It can also be observed that for PC-ABS samples etched with hexavalent chromium, the morphological parameters shown have much larger values than Evolve samples in PC-ABS, despite the fact that the latter were immersed for a longer absolute time, showing how hexavalent chromium is able to modify the morphology of PC-ABS samples more than the chemical baths without this chemical element. This observation may be able to explain several physical characteristics of such surfaces, such as a better degree of adhesion by applied glues and paints than the other surfaces studied in this work, as these morphological parameters are specifically defined in the ISO 25178 standard to predict such characteristics and the parameters shown are often used for the qualification of surfaces for this type of industrial applications.
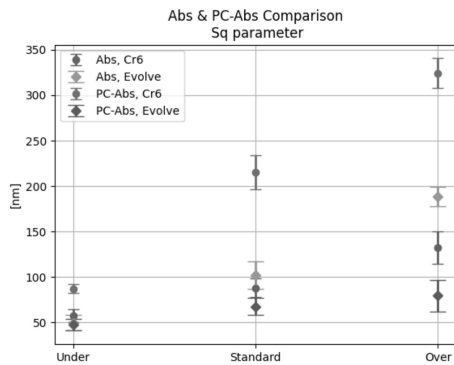

Fig. 11: The *Sq* parameter measurements for all samples studied.

If hexavalent chromium etching baths cannot be used, then the Evolve surfaces in ABS material are the most similar according to these three parameters from a morphological point of view to PC-ABS surfaces etched with hexavalent chromium. In fact, the values of these three parameters are immediately lower than the parameter values of chrome-etched PC-ABS surfaces. In addition, as can be seen from all three graphs, the *Sq*, *Sdq* and *Vv* parameters increases with the immersion time in the chemical baths: if a surface with a similar morphology of hexavalent chromium-etched PC-ABS surfaces is to be reproduced, one idea might be to increase the immersion time of the Evolve etching process for ABS surfaces. As can be seen from figures 11, 12 and 13, for example, the morphological parameters measured for Evolve samples of type "*Over*" in ABS material have values close to the values measured for the PC-ABS surfaces etched with hexavalent chromium but for "Standard" immersion times, i.e. for lower immersion times.

On the other end, the ABS surfaces etched with hexavalent chromium provided similar measurements of these three morphological parameters to the Evolve ABS surfaces, as for immersion times lower than 10 minutes, the parameters are
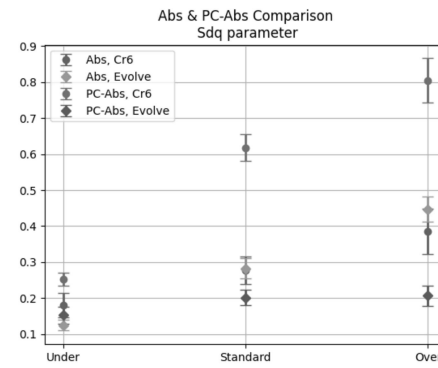

Fig. 12: The *Sdq* parameter measurements for all samples studied.

compatible regardless of the type of etching process. It is therefore preferable to use etching processes without hexavalent chromium for ABS surfaces if the use of this chemical element is to be avoided, since as just described, the morphological result obtained is similar according to these parameters.

In the end, the use of hexavalent chromium is almost indispensable for etching processes for PC-ABS surfaces. In fact, observing the values of the morphological parameters measured for the Evolve PC-ABS surfaces, it is possible to observe how the etching process does not have a great impact on the morphological characteristics of the surface: as also shown through the images of SEM, this type of surface immersed in a chemical bath without hexavalent chromium does not change radically from a morphological point of view, regardless of the immersion time of the etching process.
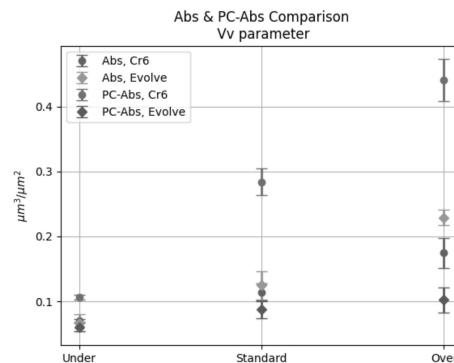

Fig. 13: The *Vv* parameter measurements for all samples studied.

VIII. CORRELATION OF PARAMETERS

In the literature, there are many studies on the possible correlation between different morphological parameters of the ISO 25178 standard. The works show that some parameters of this standard often have a correlation for certain types of surfaces: all studies propose empirical relationships and best fits found through direct measurements on the studied samples, without however proposing theoretical relationships able to explain in detail the experimental evidence. The most studied case is the possible correlation between the *Sdq* and *Sdr* hybrid parameters: observing the definitions of these parameters, it is possible to guess a possible correlation be-

tween the two, even if the existence of a real analytical correlation between the two definitions is not obvious. In Appendix A of this paper, a theoretical relation is proposed and it clearly shows how Sdr can be written as a function of Sdq, assuming that the morphology of the studied surface can be described by the isotropic Beckamann distribution of normals.

According to this assumption, it is possible to write the Sdr parameter as a function of Sdq through the relation

$$Sdr = \frac{\sqrt{\pi}}{2} \cdot Sdq \cdot \exp\left\{\frac{1}{Sdq^2}\right\} \cdot \mathrm{erfc}\left\{\frac{1}{Sdq}\right\} \qquad (12)$$

with $\mathrm{erfc}(x) = 1 - \mathrm{erf}(x)$, where $\mathrm{erf}(x)$ is the error function. In this paper, it was not studied if the Beckmann distribution adequately fits the distribution of normals observed for the studied surfaces, but it is shown that the relationship between the two parameters is evident even for etched surfaces in ABS and PC-ABS materials.

In figure 14, the values of the measured parameters of Sdq are shown on the x-axis and the values of Sdr on the y-axis. In more detail, the value of Sdq and the value of Sdr were measured for each surface studied: these two values constitute the coordinates of the points shown schematically in figure 14 representing the corresponding surfaces. The blue line is the graph of the theoretical relationship found and shown in equation (12).

The figure 14 therefore shows, without reporting a detailed statistical study in this respect, a fit of the experimental data through the theoretical relationship found, both for ABS and PC-ABS surfaces, independently of the etching process used.
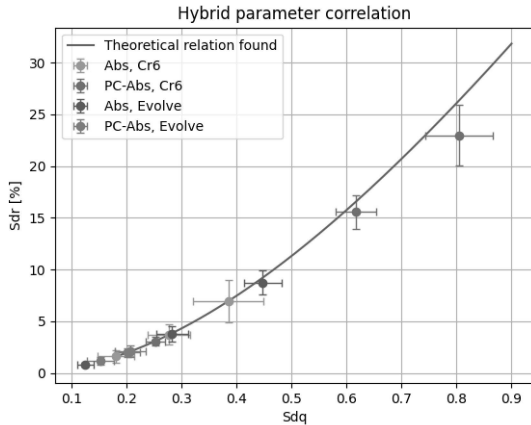

Fig. 14: The Sdr values as a function of Sdq for the studied surfaces in ABS and PC-ABS material.

Another confirmation of the theoretical relationship found can be obtained for example in the article cited here [18] in which an empirical relation obtained as a best fit is proposed through an analogous graph to the one shown in figure 14.

In the image at the top of figure 15, it is possible to observe the similar work reported in [18], in which the measurements about the parameter Sdq and Sdr and the relative best fit found are shown. In the image at the bottom of the same figure, instead, a comparison between the theoretical relation found in this work reported in equation (12) and shown in blue, and the best fit found and proposed by article [18] that

empirically correlates Sdr and Sdq parameter is shown: also in this case, without reporting a particular statistical study to compare the two relationships, it can be observed that the relationship obtained here is similar to that proposed by the work cited.
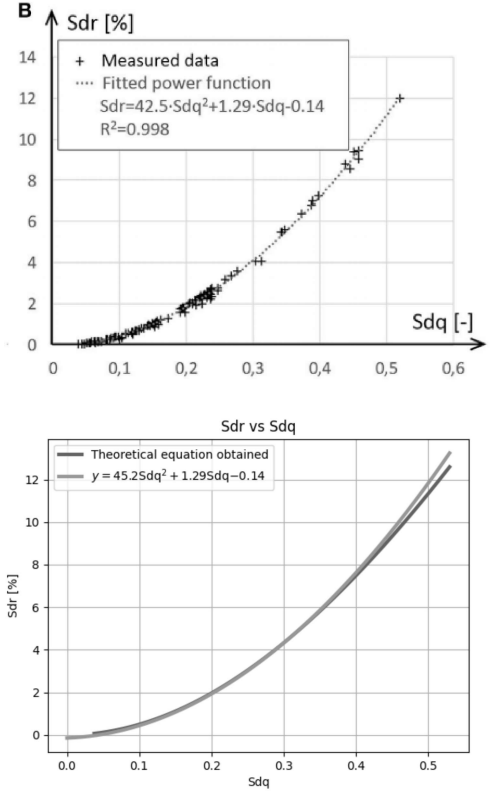

Fig. 15: On the top, the main result of the article [18], on the bottom, a comparison between the best fit found in the cited article and the theoretical relationship proposed in equation (12).

IX. CONCLUSIONS

In this paper, it was shown how the morphological parameters defined in the ISO 25178 standard can qualify ABS and PC-ABS surfaces depending on the etching process. Furthermore, the morphological differences that can be achieved depending on the type of material and the type of etching process used were described in detail.

In the end of work, the correlation between the Sdq and Sdr parameters for this type of etched surface was studied and a theoretical relationship between the Sdq parameter with the Sdr parameter was proposed, comparing this result with the measurements obtained on this type of surface and the results obtained in the literature.

A. APPENDICES

In this appendix, a mathematical demonstration of the relationship shown in equation x is provided, linking Sdr as a function of Sdq with the assumption that the morphology of the surface studied is described by the isotropic Beckmann distribution of normals in the case of continuous.

Let $f : \mathbb{R}^2 \to \mathbb{R}$ of class C^1 defined in the open set Ω and let $\vec{S_\Sigma}$ be the Cartesian surface defined as

$$\vec{S_\Sigma} = (x, y, f(x, y)) \qquad (13)$$

In this way, each measured point P_m of the scanned surface can be indicated by the surface $\vec{S_\Sigma}$ and for each of these points its normal versor

$$\hat{w}_m(\theta_m, \varphi_m) = (\sin\theta_m \cos\varphi_m, \sin\theta_m \sin\varphi_m, \cos\theta_m) \quad (14)$$

can be calculated. Let S_Σ be the area of the parametric surface $\vec{S_\Sigma}$ and let S be the area of the projection of the surface $\vec{S_\Sigma}$ on the x-y plane.

In the literature, the distribution of normals is defined in such a way that

$$a \int_0^{2\pi} \int_0^{\frac{\pi}{2}} D(\theta, \varphi) \sin\theta \, d\theta \, d\varphi = \frac{S_\Sigma}{S} \quad (15)$$

where $a = 1 \, [\text{m}^{-2}]$ is a constant that serves to bring the equation back from a dimensional point of view and it will not be reported from this point.

Using the definition of the area of a Cartesian surface, it can be shown that the definition of the Sdr parameter is equivalent to the following definition

$$Sdr = \frac{S_\Sigma}{S} - 1 \quad (16)$$

and therefore the Sdr parameter can be calculated as

$$Sdr = \int_0^{2\pi} \int_0^{\frac{\pi}{2}} D(\theta, \varphi) \sin\theta \, d\theta \, d\varphi - 1 \quad (17)$$

Similarly, given that the distribution of normals in the literature is normalised so that

$$\int_0^{2\pi} \int_0^{\frac{\pi}{2}} D(\theta, \varphi) \sin\theta \cos\theta \, d\theta \, d\varphi = 1 \quad (18)$$

On the other hand, the Sdq parameter is defined as the square root of the mean value of the square modulus of the gradient, i.e. it is defined as

$$Sdq = \sqrt{<\tan^2\theta_m>} \quad (19)$$

where θ_m is the same coordinate shown in equation (14). In this way, using the equations (18) and (19), it is possible to calculate the Sdq parameter through the distribution of normals as

$$Sdq = \sqrt{\int_0^{2\pi} \int_0^{\frac{\pi}{2}} D(\theta, \varphi) \sin\theta \cos\theta \tan^2\theta \, d\theta \, d\varphi} \quad (20)$$

If the morphology of the studied surface is described through the isotropic Beckmann distribution defined in literature as[4]

$$D(\theta, \varphi) = \frac{\exp\left\{-\frac{\tan^2\theta}{\sigma^2}\right\}}{\pi\sigma^2 \cos^4\theta} \quad (21)$$

then the integrals in equation (17) and (20) can be calculated, allowing Sdq to be obtained as

$$Sdq = \sigma \quad (22)$$

and Sdr as

$$Sdr = \frac{\sqrt{\pi}}{2} \cdot \sigma \cdot \exp\left\{\frac{1}{\sigma^2}\right\} \cdot \text{erfc}\left\{\frac{1}{\sigma}\right\} \quad (23)$$

[4] The σ quantity is a parameter that defines the morphology of the surface.

In this way, for surfaces described by the isotropic Beckmann distribution, it is possible to write Sdr as a function of Sdq as

$$Sdr = \frac{\sqrt{\pi}}{2} \cdot Sdq \cdot \exp\left\{\frac{1}{Sdq^2}\right\} \cdot \text{erfc}\left\{\frac{1}{Sdq}\right\} \quad (24)$$

The equation found is consistent from a dimensional point of view.

REFERENCES

[1] D. Lv, J. Ou, M. Xue, and F. Wang, "Stability and corrosion resistance of superhydrophobic surface on oxidized aluminum in nacl aqueous solution," *Applied Surface Science*, vol. 333, pp. 163–169, 2015.

[2] D. Chen, J. Li, J. Zhao, J. Guo, S. Zhang, T. A. Sherazi, S. Li et al., "Bioinspired superhydrophilic-hydrophobic integrated surface with conical pattern-shape for self-driven fog collection," *Journal of colloid and interface science*, vol. 530, pp. 274–281, 2018.

[3] N. Wang, D. Xiong, M. Li, Y. Deng, Y. Shi, and K. Wang, "Super-hydrophobic surface on steel substrate and its anti-icing property in condensing conditions," *Applied Surface Science*, vol. 355, pp. 226–232, 2015.

[4] G. J. Patzelt, V. Stenzel, J. Geils, and A. Stake, "Anti-icing and anticontamination properties of coatings induced by surface structure," *Journal of Coatings Technology and Research*, vol. 13, no. 4, pp. 589–596, 2016.

[5] G. D. MacAulay and C. L. Giusca, "Assessment of uncertainty in structured surfaces using metrological characteristics," *CIRP Annals*, vol. 65, no. 1, pp. 533–536, 2016.

[6] D. Yu, X. Zhong, Y. Wong, G. Hong, W. Lu, and H. Cheng, "An automatic form error evaluation method for characterizing micro-structured surfaces," *Measurement Science and Technology*, vol. 22, no. 1, p. 015105, 2010.

[7] K. E. Torrance and E. M. Sparrow, "Theory for off-specular reflection from roughened surfaces," *Josa*, vol. 57, no. 9, pp. 1105–1114, 1967.

[8] M. Oren and S. K. Nayar, "Generalization of the lambertian model and implications for machine vision," *International Journal of Computer Vision*, vol. 14, no. 3, pp. 227–251, 1995.

[9] B. Walter, S. R. Marschner, H. Li, and K. E. Torrance, "Microfacet models for refraction through rough surfaces." *Rendering techniques*, vol. 2007, p. 18th, 2007.

[10] E. Heitz, J. Hanika, E. d'Eon, and C. Dachsbacher, "Multiple-scattering microfacet bsdfs with the smith model," *ACM Transactions on Graphics (TOG)*, vol. 35, no. 4, pp. 1–14, 2016.

[11] E. Heitz and E. d'Eon, "Importance sampling microfacet-based bsdfs using the distribution of visible normals," in *Computer Graphics Forum*, vol. 33, no. 4. Wiley Online Library, 2014, pp. 103–112.

[12] E. Heitz, "Understanding the masking-shadowing function in microfacet-based brdfs," *Journal of Computer Graphics Techniques*, vol. 3, no. 2, pp. 32–91, 2014.

[13] B. Smith, "Geometrical shadowing of a random rough surface," *IEEE transactions on antennas and propagation*, vol. 15, no. 5, pp. 668–671, 1967.

[14] D. Meneveaux, B. Bringier, E. Tauzia, M. Ribardière, and L. Simonot, "Rendering rough opaque materials with interfaced lambertian micro-facets," *IEEE transactions on visualization and computer graphics*, vol. 24, no. 3, pp. 1368–1380, 2017.

[15] L. Simonot, "Photometric model of diffuse surfaces described as a distribution of interfaced lambertian facets," *Applied optics*, vol. 48, no. 30, pp. 5793–5801, 2009.

[16] "Semiconductor and dimensional metrology division; internet based surface metrology algorithm testing system (accessed on 6 july 2021)." [Online]. Available: https://physics.nist.gov/VSC/jsp/

[17] P. L. Menezes, S. V. Kailas et al., "Influence of roughness parameters on coefficient of friction under lubricated conditions," *Sadhana*, vol. 33, no. 3, p. 181, 2008.

[18] Á. Czifra and I. Bárányi, "Sdq-sdr topological map of surface topographies," *Frontiers in Mechanical Engineering*, vol. 6, p. 50, 2020.